



Data
Models
Inventories

PARIS

Process Attribution of Regional Emissions

GA 101081430, RIA

Complete calendar year of extended and quality-controlled
APO data uploaded to the ICOS portal

Milestone M43

Delivery due date Annex I	PM 27		
Actual date of submission	PM 36		
Lead beneficiary: UNIVBRIS	Work package: WP6	Nature: R	Dissemination level: PU
Responsible scientist	Matt Rigby		
Contributors	Karina Adcock, Penelope Pickers, Eric Saboya		
Internal reviewers	-		
Version: 1			



Horizon Europe Cluster 5: Climate, energy and mobility

"This project has received funding from the European Union's Horizon Europe Research and Innovation programme under HORIZON-CL5-2022-D1-02 Grant Agreement No 101081430 - PARIS".



Data
Models
Inventories

M43 – Complete calendar year of extended and quality-controlled APO data uploaded to the ICOS portal

Table of content

1. CHANGES WITH RESPECT TO THE DOA (DESCRIPTION OF THE ACTION)	3
2. SUMMARY	3
3. MEASUREMENT METHODOLOGY	3
4. MEASUREMENT UNCERTAINTIES	5
5. ESTIMATING FOSSIL FUEL CO₂ MOLE FRACTIONS	7
6. ATMOSPHERIC MODELLING OF APO AND FFCO₂	7
7. APO INVERSION METHODOLOGY	8
8. FORWARD SIMULATIONS AND INVERSION UNCERTAINTIES	10
9. REFERENCES	11
10. HISTORY OF THE DOCUMENT	14

1. Changes with respect to the DoA (Description of the Action)

Milestone M43 has been added to the DoA in the context of the 2nd Amendment of the Grant Agreement. It describes the methodology and uncertainties associated with the data production and inverse estimates which are part of deliverable D6.2. The deliverable will cover the APO data uploaded to the ICOS portal through 2024, and associated products derived from the data. The deliverable report will provide a brief overview of the uploaded data and a brief description of the data and metadata. It will include an overview of progress towards producing robust fossil fuel CO₂ mole fraction timeseries, and top-down fossil fuel CO₂ flux estimates based on APO data (including tabulated values, where quality standards are met).

2. Summary

This report describes the methodology underpinning high-frequency atmospheric measurements of carbon dioxide and oxygen at Weybourne Atmospheric Observatory and Heathfield Tower in the UK. Furthermore, it describes the status of development of the PARIS methodology for inferring fossil fuel CO₂ fluxes from such data. Preliminary comparisons of the data and model are presented. Information on the archival of the data and preliminary flux estimates are presented in the associated Deliverable Report (D6.2).

3. Measurement methodology

Carbon dioxide (CO₂) and oxygen (O₂) vary in the atmosphere due to a range of processes including terrestrial biosphere exchange, combustion (e.g. fossil fuels and wild fires) and air–sea gas exchange with the oceans. Terrestrial biosphere fluxes of O₂ and CO₂ are strongly anti-correlated, with a stoichiometric exchange ratio of 1.05–1.10 moles of O₂ consumed per mole of CO₂ produced (or vice versa) (Severinghaus, 1995; Keeling and Manning, 2014). In fossil fuel combustion O₂ is consumed, and CO₂ is produced, with a globally weighted average stoichiometric exchange ratio of about 1.38 mol mol⁻¹ (Keeling and Manning, 2014). There is no fixed stoichiometric coupling between CO₂ and O₂ in ocean–atmosphere fluxes due to their different seawater chemistry properties (Keeling et al., 1993). Due to these varied relationships between CO₂ and O₂, measuring atmospheric O₂ concurrently to CO₂ provides a wealth of additional information on carbon biogeo-chemical cycles than can be achieved by measuring CO₂ alone.

Here, we present continuous in-situ atmospheric time series of CO₂ and O₂ from two measurement stations in the UK: Weybourne Atmospheric Observatory (WAO), Norfolk (52.95°N, 1.12°E) starting in 2010; and Heathfield Tower (HFD), Sussex (50.98°N, 0.23°E) starting in 2021. These stations both use measurement systems with the same design.

The measurement system alternates sampling air between two inlet lines every 2 hours. Each inlet line includes an aspirated air inlet. At Weybourne the inlets are approximately 10 m above ground level and at Heathfield they are approximately 100 m. Air from the inlets passes through a two-stage drying system, which prevents dilution effects caused by water vapour. Stage one is a thermo-electric cooler set at approximately 1 °C, and stage two is a cryogenic cooler set at approximately –80 °C.

M43 – Complete calendar year of extended and quality-controlled APO data uploaded to the ICOS portal

The atmospheric CO_2 mole fraction is measured by a non-dispersive infrared (NDIR) CO_2 analyser from Siemens Corp., model Ultramat 6E and the atmospheric O_2 mole fraction is measured by an "Oxzilla", a dual fuel cell O_2 analyser from Sable Systems International Inc. The Ultramat and Oxzilla analysers are both differential analysers and are placed in series. A cylinder containing dry ambient air is continuously run through the reference side of the differential Ultramat and Oxzilla analysers (Figure 1).

The measurement system produces an O_2 and CO_2 measurement every 2 minutes. These data are then reported as hourly averages. Gaps in the data are due to routine running of calibration cylinders, maintenance and removal of data with known technical issues. A full description of the Weybourne measurement system is provided in Adcock et al. (2023).

A suite of three or four cylinders with mole fractions spanning the typical range observed at the station, is used to calibrate the analysers every 47 hours. The O_2 and CO_2 mole fractions in the cylinders are pre-determined by measuring the cylinders, against a suite of primary standards obtained from NOAA (National Oceanic and Atmospheric Administration), USA and Scripps Institution of Oceanography (SIO). The CO_2 data are transferred onto the World Meteorological Organization (WMO) NOAA X2019 calibration scale using the linear conversion in Hall et al., (2021). The O_2 data are reported on the SIO "S2" scale that was used by SIO from April 1995 to August 2017 (Keeling et al., 2020).

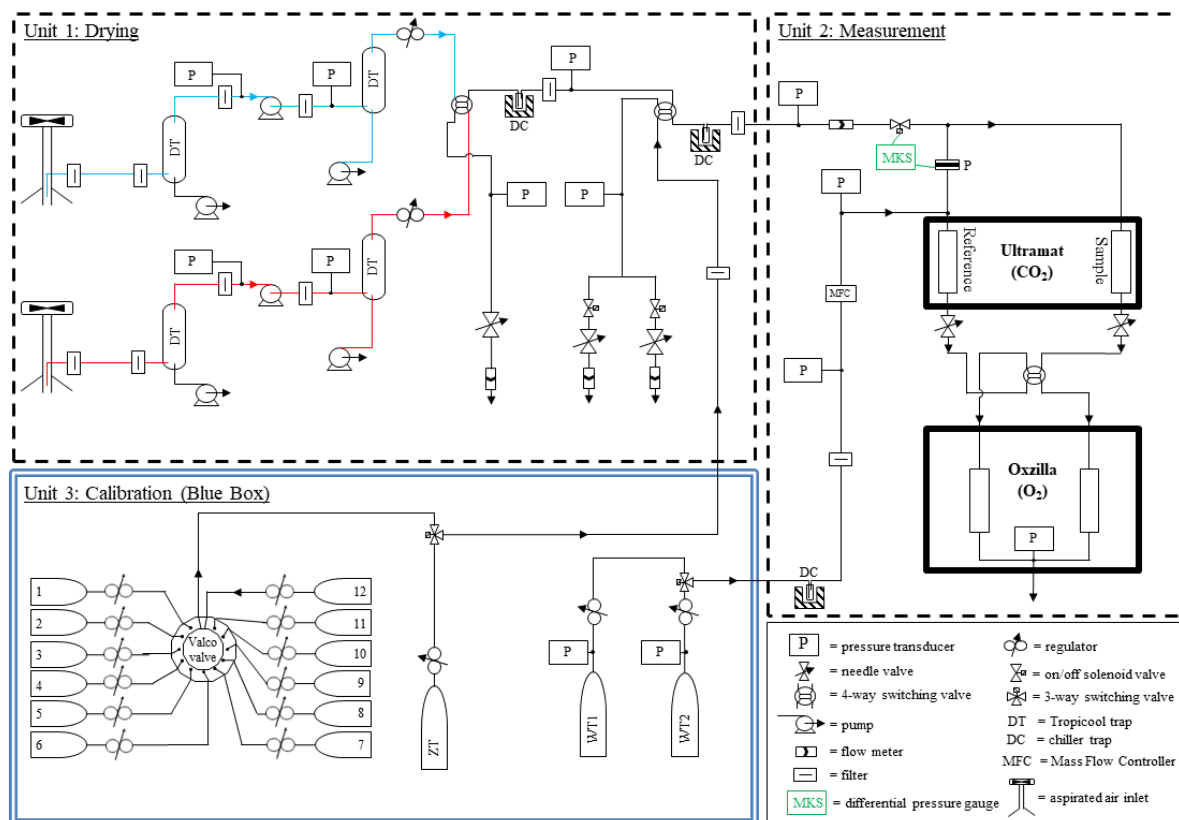


Figure 1: Gas handling diagram of the Weybourne Atmospheric Observatory (WAO) O_2 and CO_2 measurement system.

4. Measurement uncertainties

The uncertainty of the measurements can be accessed in multiple different ways. Firstly, a Target Tank (TT) is typically measured every 11 hours as a quality control check on both the measurement system and the calibration procedures. Adcock et al. (2023) found at Weybourne an overall compatibility for CO₂ is -0.037 ± 0.146 ppm and for O₂ is 0.5 ± 4.4 per meg. For comparison, the WMO compatibility goals are ± 0.1 ppm for CO₂ in the Northern Hemisphere and ± 2 per meg (aspirational) and ± 10 per meg (extended) for O₂ globally (Crotwell et al., 2020).

Figures 2 and 3 show the hourly standard deviations of the two-minute measurements at Weybourne and Heathfield. These standard deviations include both the uncertainty in the measurement system and how much the actual CO₂ and O₂ mole fractions in the air vary in an hour. Therefore, these standard deviations cannot be compared to the Target Tanks or to the WMO goals. The $\pm 1\sigma$ standard deviation of the CO₂ measurements is very stable over time. On average at Weybourne, the CO₂ standard deviation is $\pm 0.09 \pm 0.11$ ppm and the O₂ standard deviation is $\pm 6.5 \pm 5.1$ per meg. On average at Heathfield, the CO₂ standard deviation is $\pm 0.11 \pm 0.12$ ppm and the O₂ standard deviation is $\pm 8.2 \pm 10.7$ per meg. However, the O₂ standard deviations are more variable and have periods of much larger standard deviations due to poorer performance of the Oxzilla analyser.

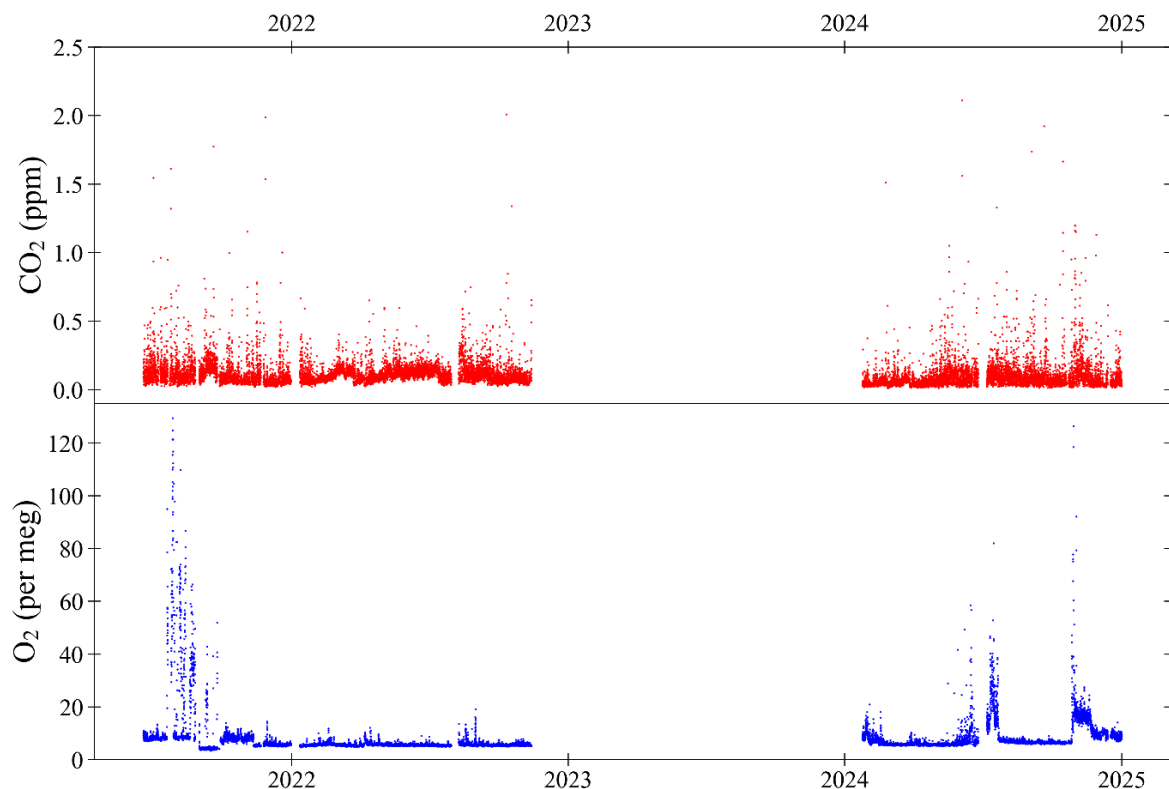


Figure 2: CO₂ and O₂ hourly standard deviations of the 2-minute atmospheric measurements at Heathfield Tower (HFD).

M43 – Complete calendar year of extended and quality-controlled APO data uploaded to the ICOS portal

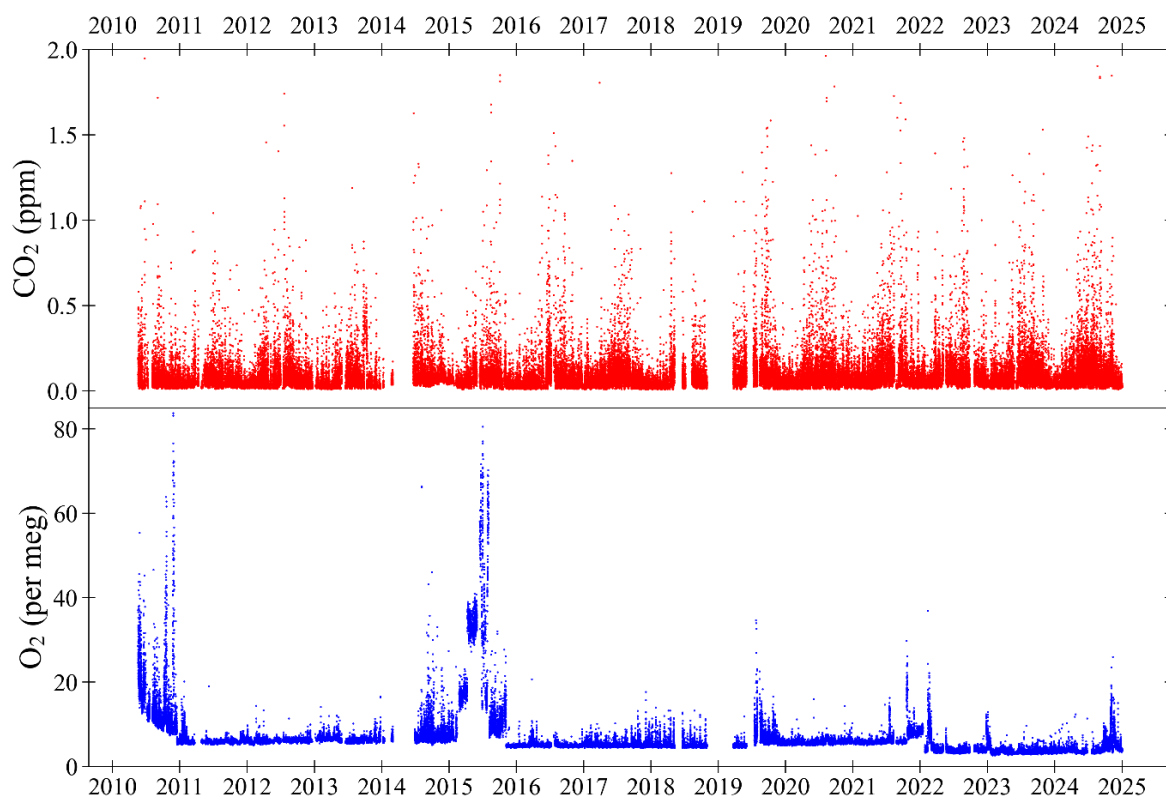


Figure 3: CO₂ and O₂ hourly standard deviations of the 2-minute atmospheric measurements at Weybourne Atmospheric Observatory (WAO).

Weybourne has participated in three intercomparison programmes to assess its compatibility with other atmospheric measurement sites. These intercomparison programmes are: "Cucumbers" (<http://www.cucumbers.uea.ac.uk>); "GOLLUM" (Global Oxygen Laboratories Link Ultra-precise Measurements, <http://www.gollum.uea.ac.uk>); and the WMO/IAEA Round Robin Comparison Experiment (World Meteorological Organization/International Atomic Energy Agency, <http://gml.noaa.gov/ccgg/wmor/index.html>).

These intercomparison programmes involve measuring the chemical composition of gas in the same cylinders, circulated amongst different laboratories and comparing the measurements to assess the laboratory inter-compatibility. The average offsets at WAO relative to the initial central laboratory analysis are shown in Table 1.

Table 1: The average offsets at WAO relative to the initial central laboratory analysis for the three intercomparison programmes WAO participated in. These average offsets are the average of the cylinder differences and the $\pm 1\sigma$ standard deviation of the cylinder differences.

Intercomparison programme	CO ₂ (ppm)	O ₂ (per meg)
GOLLUMs	-0.04 ± 0.11	-0.5 ± 6.0
Cucumbers	-0.11 ± 0.15	5.8 ± 12.3
WMOs	-0.22 ± 0.08	-2.6 ± 2.6

5. Estimating fossil fuel CO₂ mole fractions

Atmospheric measurements of O₂ and CO₂ can be combined into a tracer known as Atmospheric Potential Oxygen (APO = O₂ + 1.1 × CO₂), which is expected to be invariant to terrestrial biosphere exchange. The coefficient 1.1 represents the mean molar O₂:CO₂ exchange ratio of the terrestrial biosphere. Variability in APO therefore reflects mostly ocean-atmosphere exchange and fossil fuel combustion. If ocean-atmosphere exchange is small, regional fossil fuel CO₂ signals can be isolated by subtracting a "clean air" APO baseline that incorporates the oceanic variations (Pickers, 2016). If we let ffCO₂ denote regional fossil fuel signals. Then

$$ffCO_2 = \frac{APO - APO_{bl}}{R_{APO}},$$

where APO_{bl} denotes the APO "baseline" and R_{APO} is the mean molar ratio (R) of APO:CO₂ for fossil fuel emissions.

R_{APO} can also be thought of as the measured O₂:CO₂ ratio minus the biospheric O₂:CO₂ ratio (O₂:CO_{2meas} – O₂:CO_{2bio}). R_{APO} can be calculated in several ways: in its simplest form a constant value can be used. Assuming the measured CO₂ is coming from fossil fuels it likely has a ratio of about 1.4, then assuming biospheric exchange is 1.1, this gives a R_{APO} ratio of 0.3. For example, Pickers et al. (2022) used 0.37. In Pickers et al. (2022) this R_{APO} was generated from the COFFEE (CO₂ release and oxygen uptake from fossil fuel emission estimate) gridded database (Steinbach et al., 2011).

The APO baseline are values that are representative of the well-mixed troposphere, far from the influence of sources and sinks. These can be calculated using a statistical baseline fitting method (e.g. Pickers et al., 2022; Chawner et al., 2024) or a suitable up-wind background station with APO data, if available. Within PARIS the focus is on using inverse modelling techniques to quantify ffCO₂ (see further details below).

Pickers et al. (2022) estimated an hourly ffCO₂ uncertainty of ±42%, which is dominated by the uncertainty in R_{APO}, followed by the uncertainty in the APO baseline.

6. Atmospheric modelling of APO and ffCO₂

The UK Met Office NAME model was used to simulate the transport of APO or ffCO₂ to the atmospheric measurement stations (Numerical Atmospheric dispersion Modelling Environment v8.2; Jones et al., 2007). NAME was run in time-reversed mode to quantify the sensitivity of atmospheric mole fractions to potential fluxes (so-called "footprints"), within a regional domain, as described in White et al. (2019). The European domain covers 98°W–40°E longitude and 11°N–77°N, with footprints archived at 0.352° x 0.234° resolution, and generated for 1-hourly averaged observations. Outside of the model region, boundary conditions are taken from global 3D models (described below).

Figure 4 shows a comparison between NAME-simulated ffCO₂ and that derived from atmospheric CO₂ and O₂ measurements at WAO. The NAME simulations used fossil fuel flux fields from the 2022 High Resolution Carbon-Tracker Europe product (CTE-HR; Van der Woude et al., 2023).

M43 – Complete calendar year of extended and quality-controlled APO data uploaded to the ICOS portal

These simulations were reported in the PARIS Milestone 24 report and generally show larger variability in the observation-derived ffCO_2 than in the model simulations. These findings either indicate substantially larger fossil fuel CO_2 fluxes than in CTE-HR, or the influence of errors in APO boundary conditions and/or the influence of coastal fluxes. These model-data differences are the subject of ongoing investigation, including through the development of more formal inverse modelling protocols, as outlined in the following section.

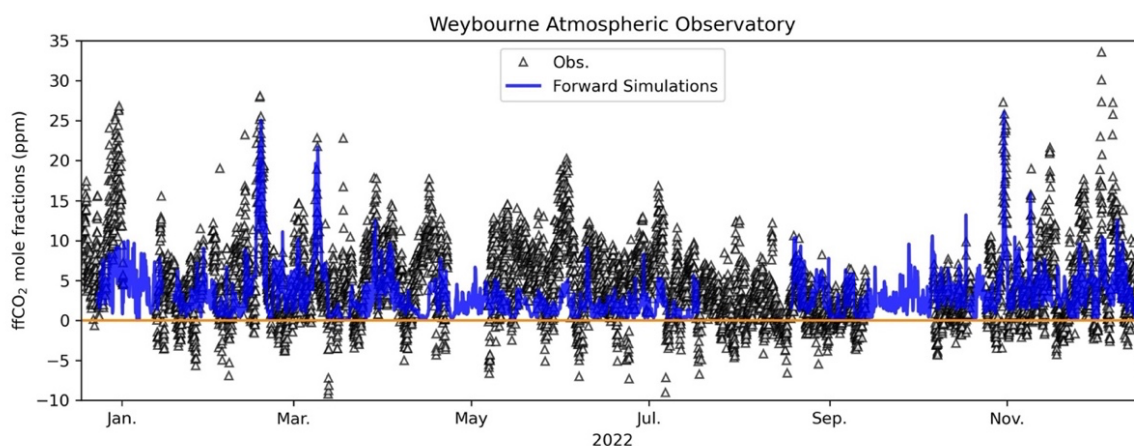


Figure 4: NAME-simulated ffCO_2 at Weybourne Atmospheric Observatory during 2022 (blue), compared to that derived from atmospheric observations (black triangles). Reproduced from the PARIS Milestone 24 report.

7. APO inversion methodology

The process of inferring emissions from atmospheric mole fraction data, or tracers derived from such observations (e.g. APO), is known as inverse modelling. Typically, a Bayesian approach is used in which a priori flux estimates are combined with an atmospheric chemical transport model to make an initial prediction of the observations. The fluxes are then adjusted to bring the model and data into closer agreement, with the two sources of information weighted by their relative uncertainties.

For the PARIS APO inversions, the NAME European modelling domain is split into 55 scaling regions (basis functions) for each flux sector. The scaling regions over Europe are not spatially fixed and are recalculated for each month. Scaling regions in the rest of the inversion domain are always spatially fixed. The geographical coverage of each scaling region in Europe is calculated from multiplying the mean footprint field with the converging estimated absolute flux field for each month. The inversion domain is split (with land and sea areas kept distinct in each scaling region) such that summing the grid cells in each scaling region yields approximately the same footprint-flux value. Scaling regions closer to the measurement stations encompass fewer grid cells (and a smaller geographical area) than those much further away which encompass larger geographical areas.

Inversions are performed using the Regional Hierarchical Inverse Modelling Environment (RHIME), which has been frequently used for regional trace gas inversions of various atmospheric species across the globe (e.g., Ganesan et al., 2014; Say et al., 2021; Western et al., 2022). RHIME uses a MCMC (Markov Chain Monte Carlo) approach to quantify a mean

M43 – Complete calendar year of extended and quality-controlled APO data uploaded to the ICOS portal

multiplicative scaling (with confidence intervals) of a priori fluxes for each sector of interest.

The PARIS inversions are performed in “APO-space” (as in Rodenbeck et al. 2023), where sectoral flux field estimates for CO₂ and O₂ are combined to create APO flux fields. Only fossil fuel and ocean APO fluxes were used in the model since, by construction, there are theoretically no APO fluxes from the terrestrial biosphere.

Fossil fuel fluxes of CO₂, $F_f^{CO_2}$, are related to O₂ fluxes, $F_f^{O_2}$, by their molar exchange ratio, α_f such that

$$F_f^{O_2} = -\alpha_f F_f^{CO_2}.$$

From the definition of APO and the above equation, the fossil fuel APO flux field is defined as

$$F_f^{APO} = -(\alpha_f + \alpha_l) F_f^{CO_2}.$$

Here, α_l is the CO₂:O₂ molar exchange ratio for the land biosphere and takes a value of 1.1. Monthly fossil fuel CO₂ fluxes from EDGAR v8.0 (Crippa et al., 2021) were combined with fossil fuel CO₂:O₂ molar exchange ratios from the GridFED v2024 database (Jones et al. 2021) to construct fossil fuel APO flux fields. EDGAR provides 0.10°x0.10° global anthropogenic CO₂ emissions estimates from 1970-2023 which were regridded using a mass-conservation approach to match the NAME footprint domain and spatial resolution. For 2024, the 2023 emissions field was used.

Ocean APO fluxes were similarly constructed from flux fields of CO₂, O₂, and N₂. Keeling and Manning (2014) demonstrated that a first order approximation of $\delta(O_2/N_2)$ oceanic fluxes can be modelled as

$$Z_{eff} = Z_{O_2} - \frac{X_{O_2}}{X_{N_2}} \times Z_{N_2}.$$

Here, Z_{O_2} and Z_{N_2} are the respective O₂, and N₂ net ocean-atmosphere flux exchanges. X_{O_2} and X_{N_2} are the reference oxygen and nitrogen standard values, respectively. A value of 0.79019 is used for X_{N_2} .

Combined with the net ocean-atmosphere CO₂ flux exchange, Z_{CO_2} , we can model oceanic APO fluxes as

$$F_{ocean}^{APO} = Z_{eff} - \alpha_l Z_{CO_2}.$$

Similar to Chawner et al. (2024), we used oceanic CO₂, O₂, and N₂ flux fields from NEMO-ERSEM (Butenschön et al., 2016; Madec and NEMO System Team, 2022), which were combined into an APO oceanic flux following the above equation for ocean APO fluxes. The NEMO-ERSEM ocean fluxes have a daily time resolution and raw spatial resolution of 0.066°x0.110°, which were also regridded using a mass-conservation approach to match the NAME domain and spatial resolution. Since NEMO-ERSEM fluxes were only available until 2015, we used the 2015 fluxes to model the oceanic APO fluxes for 2022-2024.

As the focus of this study was to use APO observations to constrain land-based fossil fuel CO₂ emissions estimates, using an outdated version of the ocean fluxes is less problematic

provided a sufficiently large uncertainty is assigned to these fluxes in the inversion, and the ocean and land parts of the inversion domain are optimised using separate basis functions with distinct land and sea areas that do not overlap. Furthermore, we did not find a statistically significant trend in the NEMO-ERSEM ocean fluxes in the model domain over 2005-2015 (the period we had data available).

The Jena Carboscope (JC) inverse model (Rodenbeck et al. 2023) produced daily global estimates of APO values for 2002-2021 from global inversions of APO observations from 11 global stations and ship measurements (JC version "apo99XS_v2022"). The global stations used in this model do not include any of the ICOS measurement stations used in the RHIME regional inversion.

The JC APO values were extrapolated to 2024 at three latitudinal bands (30°N-90°N; 30°S-30°N; 90°S-30°S) using a linear regression applied to the 2017-2021 APO values. From this linear regression, we detrended the JC APO values and propagated the 2017-2021 mean APO seasonal cycle forwards in time to provide daily APO value estimates for 2022-2024. Whilst extrapolation can introduce large uncertainties into the data and is generally not recommended, this was the best approach available at the time.

The JC APO values formed the boundary condition fields along the edges of the NAME model domain for each month. Boundary conditions were calculated using the NAME particle density at the edge of the model domain. A scaling was calculated for each cardinal boundary in each 1-month period of inference to derive posterior boundary condition values.

8. Forward simulations and inversion uncertainties

During the development and testing phase of the PARIS APO inversions, we used a setup similar to the inversions that we had developed using APO and radiocarbon CO₂ data during the CORSO project (CO2MVS Research on Supplementary Observations; 2022 - 2025). Here, rather than using the HFD and WAO high-frequency data, we used flask samples collected by the Integrated Carbon Observing System (ICOS RI, 2025). This approach allowed us to efficiently test the system, given the lower computational cost of assimilating low-frequency flask samples, compared to high-frequency data, and will allow us to compare to fossil fuel CO₂ fluxes to those derived from radiocarbon observations collected in a similar set of flask samples. Once the methodology has been proven using these measurements, it will be adapted to the PARIS high-frequency data.

An APO timeseries compared to ICOS flask samples at Cabauw, Netherlands is shown in Figure 5. The prior simulation is generally lower than the observations, primarily due an offset with the JC boundary conditions. This offset is corrected in the inversion and does not have a strong influence on regional flux estimates. However, consistent with the ffCO₂ model-data comparison in Figure 4, the dynamic range in the detrended observations is also substantially larger than that of the model (note that the gradient in the regression line differs from the 1:1 line by approximately a factor of 2). As with the ffCO₂ comparison at WAO, this difference either implies substantially larger regional fossil fuel CO₂ emissions than in the prior fluxes (this time from EDGAR v8.2), or the influence of some other factor such as coastal fluxes, or incorrect specification of CO₂:O₂ exchange ratios.

M43 – Complete calendar year of extended and quality-controlled APO data uploaded to the ICOS portal

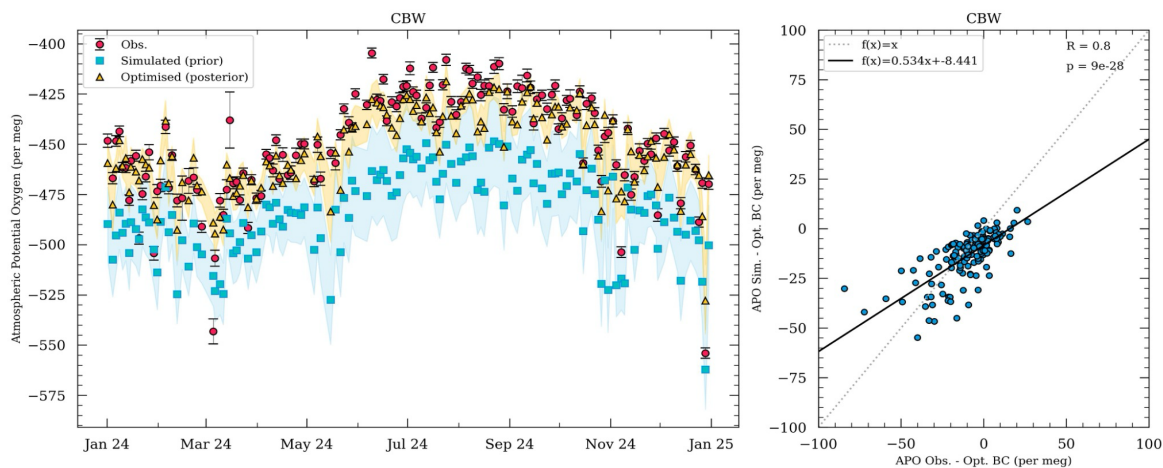


Figure 5: APO calculated from CO₂ and O₂ observations at Cabauw, Netherlands (CBW; red circles), compared to a priori NAME simulations (blue squares) and APO simulated using optimised fluxes (yellow triangles). The timeseries is shown on the left, and the detrended model-data comparison is shown as a scatter plot on the right.

In the PARIS APO inversions using the ICOS data, we estimated the model uncertainty as being equal to the mean residual between the prior simulation and the observations. The model-data uncertainties were calculated as the sum in quadrature of the observational uncertainty and this model uncertainty. The uncertainty on the prior fluxes was arbitrarily assumed to be 35% on each spatial basis function for fossil fuel fluxes, and 600% for the ocean regions. These uncertainties are propagated through the inversion, assuming a truncated Gaussian distribution on the prior, to provide a posterior flux estimate on the fossil and ocean fluxes. Preliminary results are provided in PARIS Deliverable Report 6.2.

9. References

- Adcock, K. E., Pickers, P. A., Manning, A. C., Forster, G. L., Fleming, L. S., Barningham, T., Wilson, P. A., Kozlova, E. A., Hewitt, M., Etchells, A. J., and Macdonald, A. J.: 12 years of continuous atmospheric O₂, CO₂ and APO data from Weybourne Atmospheric Observatory in the United Kingdom, *Earth Syst. Sci. Data*, 15, 5183–5206, <https://doi.org/10.5194/essd-15-5183-2023>, 2023.
- Butenschön, M., Clark, J., Aldridge, J. N., Icarus Allen, J., Artioli, Y., Blackford, J., Bruggeman, J., Cazenave, P., Ciavatta, S., Kay, S., Lessin, G., van Leeuwen, S., van der Molen, J., de Mora, L., Polimene, L., Sailley, S., Stephens, N., & Torres, R. (2016). ERSEM 15.06: A generic model for marine biogeochemistry and the ecosystem dynamics of the lower trophic levels. *Geoscientific Model Development*, 9(4). <https://doi.org/10.5194/gmd-9-1293-2016>
- Chawner, H., Saboya, E., Adcock, K. E., Arnold, T., Artioli, Y., Dylag, C., Forster, G. L., Ganesan, A., Graven, H., Lessin, G., Levy, P., Luijkx, I. T., Manning, A., Pickers, P. A., Rennick, C., Rödenbeck, C., & Rigby, M. (2024). Atmospheric oxygen as a tracer for fossil fuel carbon dioxide: a sensitivity study in the UK. *Atmospheric Chemistry and Physics*, 24(7), 4231–4252. <https://doi.org/10.5194/acp-24-4231-2024>

M43 – Complete calendar year of extended and quality-controlled APO data uploaded to the ICOS portal

Chawner, H., Saboya, E., Adcock, K. E., Arnold, T., Artioli, Y., Dylag, C., Forster, G. L., Ganesan, A., Graven, H., Lessin, G., Levy, P., Luijkx, I. T., Manning, A., Pickers, P. A., Rennick, C., Rödenbeck, C., and Rigby, M.: Atmospheric oxygen as a tracer for fossil fuel carbon dioxide: a sensitivity study in the UK, *Atmos. Chem. Phys.*, 24, 4231–4252, <https://doi.org/10.5194/acp-24-4231-2024>, 2024.

Crippa, M., Guizzardi, D., Solazzo, E., Muntean, M., Schaaf, E., Monforti-Ferrario, F., Banja, M., Olivier, J. G. J., Grassi, G., Rossi, S., & Vignati, E. (2021). GHG emissions of all world countries - 2021 Report. In *Publications Office of the European Union* (Issue October).

Crotwell, A., Lee, H., and Steinbacher, M. (Eds.): 20th WMO/IAEA Meeting on Carbon Dioxide, Other Greenhouse Gases and Related Measurement Techniques (GGMT-2019), Global Atmosphere Watch (GAW) Report No. 255, Jeju Island, South Korea, https://library.wmo.int/doc_num.php?explnum_id=10353, 2020.

ICOS RI, Apadula, F., Arnold, S., Bergamaschi, P., Biermann, T., Chen, H., Colomb, A., Conil, S., Couret, C., Cristofanelli, P., De Mazière, M., Delmotte, M., Di Iorio, T., Emmenegger, L., Forster, G., Frumau, A., Harris, E., Haszpra, L., Hatakka, J., Heliasz, M., Heltai, D., Hensen, A., Hermansen, O., Hoheisel, A., Kneuer, T., Komínková, K., Kubistin, D., Larmanou, E., Laurent, O., Laurila, T., Lehner, I., Lehtinen, K., Leskinen, A., Leuenberger, M., Levula, J., Lindauer, M., Lopez, M., Lund Myhre, C., Lunder, C., Mammarella, I., Manca, G., Manning, A., Marek, M.V., Marklund, P., Meinhardt, F., Miettinen, P., Molnár, M., Montaguti, S., Mölder, M., Müller-Williams, J., O'Doherty, S., Ottosson-Löfvenius, M., Piacentino, S., Pichon, J.-M., Pitt, J., Platt, S.M., Plaß-Dülmer, C., Ramonet, M., Rivas-Soriano, P., Roulet, Y.-A., Scheeren, B., Schmidt, M., Schumacher, M., Sferlazzo, D., Sha, M.K., Smith, P., Stanley, K., Steinbacher, M., Sørensen, L.L., Trisolino, P., Vitková, G., Ylisirniö, A., Yver-Kwok, C., Zazzeri, G., Zwerschke, E., di Sarra, A., ICOS ATC-Laboratoires des Sciences du Climat et de L'Environnement (LSCE), France, ICOS Central Radiocarbon Laboratory (CRL), Germany, ICOS Flask And Calibration Laboratory (FCL), Germany, 2025. ICOS Atmosphere Release 2025-1 of Level 2 Greenhouse Gas Mole Fractions of CO₂, CH₄, N₂O, CO, meteorology and 14CO₂, and flask samples analysed for CO₂, CH₄, N₂O, CO, H₂, SF₆, delta 13C CO₂, delta18OCO₂, delta O₂N₂ and 14C. <https://doi.org/10.18160/PP29-9CNZ>

Jones, A., Thomson, D., Hort, M., & Devenish, B. (2007). The U.K. Met Office's Next-Generation Atmospheric Dispersion Model, NAME III. In *Air Pollution Modeling and Its Application XVII* (pp. 580–589). Springer US. https://doi.org/10.1007/978-0-387-68854-1_62

Jones, M. W., Andrew, R. M., Peters, G. P., Janssens-Maenhout, G., De-Gol, A. J., Ciais, P., Patra, P. K., Chevallier, F., & Le Quéré, C. (2021). Gridded fossil CO₂ emissions and related O₂ combustion consistent with national inventories 1959–2018. *Scientific Data*, 8(1). <https://doi.org/10.1038/s41597-020-00779-6>

Ganesan, A. L., Rigby, M., Zammit-Mangion, A., Manning, A. J., Prinn, R. G., Fraser, P. J., Harth, C. M., Kim, K. R., Krummel, P. B., Li, S., Mühle, J., O'Doherty, S. J., Park, S., Salameh, P. K., Steele, L. P., & Weiss, R. F. (2014). Characterization of uncertainties in atmospheric trace gas inversions using hierarchical Bayesian methods. *Atmospheric Chemistry and Physics*, 14(8). <https://doi.org/10.5194/acp-14-3855-2014>

M43 – Complete calendar year of extended and quality-controlled APO data uploaded to the ICOS portal

Hall, B. D., Crotwell, A. M., Kitzis, D. R., Mefford, T., Miller, B. R., Schibig, M. F., and Tans, P. P.: Revision of the World Meteorological Organization Global Atmosphere Watch (WMO/GAW) CO₂ calibration scale, *Atmos. Meas. Tech.*, 14, 3015–3032, <https://doi.org/10.5194/amt-14-3015-2021>, 2021.

Keeling and Manning, Studies of Recent Changes in Atmospheric O₂ Content. In: *Treatise on Geochemistry (Second Edition)*, Holland, H. D. and Turekian, K. K. (Eds.), Elsevier, Oxford, <https://doi.org/10.1016/B978-0-08-095975-7.00420-4>, 2014.

Keeling, R. F., Walker, S. J., & Paplawsky, W.: Span Sensitivity of Scripps Interferometric Oxygen Analyzer. UC San Diego: Scripps Institution of Oceanography. Retrieved from <https://escholarship.org/uc/item/7tt993fj>, 2020.

Keeling, R. F., Najjar, R. P., Bender, M. L., and Tans, P. P.: What atmospheric oxygen measurements can tell us about the global carbon cycle, *Global Biogeochem. Cycles*, 7, 37–67, <https://doi.org/10.1029/92gb02733>, 1993.

Madec, G. and NEMO System Team: NEMO ocean engine, Zenodo, <https://doi.org/10.5281/zenodo.1464816>, 2022.

Pickers, New applications of continuous atmospheric O₂ measurements: meridional transects across the Atlantic Ocean, and improved quantification of fossil fuel - derived CO₂, *PhD thesis, University of East Anglia*, 2016.

Pickers, P.A., Manning, A.C., Le Quéré, C., Forster, G.L., Lujkx, I.T., Gerbig, C., Fleming, L.S. and Sturges, W.T.: Novel quantification of regional fossil fuel CO₂ reductions during COVID-19 lockdowns using atmospheric oxygen measurements, *Sci. Adv.*, 8, <https://doi.org/10.1126/sciadv.abl9250>, 2022.

Rödenbeck, C., Adcock, K. E., Erritt, M., Gachkivskyi, M., Gerbig, C., Hammer, S., Jordan, A., Keeling, R. F., Levin, I., Maier, F., Manning, A. C., Moossen, H., Munassar, S., Pickers, P. A., Rothe, M., Tohjima, Y., and Zaehle, S.: The suitability of atmospheric oxygen measurements to constrain western European fossil-fuel CO₂ emissions and their trends, *Atmos. Chem. Phys.*, 23, 15767–15782, <https://doi.org/10.5194/acp-23-15767-2023>, 2023

Say, D., Manning, A. J., Western, L. M., Young, D., Wisher, A., Rigby, M., Reimann, S., Vollmer, M. K., Maione, M., Arduini, J., Krummel, P. B., Mühle, J., Harth, C. M., Evans, B., Weiss, R. F., Prinn, R. G., & O'Doherty, S. (2021). Global trends and European emissions of tetrafluoromethane (CF₄), hexafluoroethane (C₂F₆) and octafluoropropane (C₃F₈). *Atmospheric Chemistry and Physics*, 21(3). <https://doi.org/10.5194/acp-21-2149-2021>

Severinghaus, J. P.: Studies of the Terrestrial O₂ and Carbon Cycles in Sand Dune Gases and in Biosphere, *PhD thesis, Columbia University*, <https://doi.org/10.2172/477735>, 1995.

Steinbach, J., Gerbig, C., Rödenbeck, C., Karstens, U., Minejima, C., and Mukai, H.: The CO₂ release and Oxygen uptake from Fossil Fuel Emission Estimate (COFFEE) dataset: effects from varying oxidative ratios, *Atmos. Chem. Phys.*, 11, 6855–6870, <https://doi.org/10.5194/acp-11-6855-2011>, 2011. van der Woude, A. M., de Kok, R., Smith, N., Lujkx, I. T., Botia, S., Karstens, U., Kooijmans, L. M. J., Koren, G., Meijer, H. A. J., Steeneveld, G.-J., Storm, I., Super, I., Scheeren, H. A., Vermeulen, A., Peters, W., Van der Woude, A. M., de Kok, R., Smith, N., Lujkx, I. T., ... Peters, W. (2023). Near-real-time CO₂ fluxes from



Data
Models
Inventories

M43 – Complete calendar year of extended and quality-controlled APO data uploaded to the ICOS portal

CarbonTracker Europe for high-resolution atmospheric modeling. *Earth System Science Data*, 15(2), 579–605. <https://doi.org/10.5194/essd-15-579-2023>

Western, L. M., Redington, A. L., Manning, A. J., Trudinger, C. M., Hu, L., Henne, S., Fang, X., Kuijpers, L. J. M., Theodoridi, C., Godwin, D. S., Arduini, J., Dunse, B., Engel, A., Fraser, P. J., Harth, C. M., Krummel, P. B., Maione, M., Mühle, J., O'Doherty, S., ... Rigby, M. (2022). A renewed rise in global HCFC-141b emissions between 2017-2021. *Atmospheric Chemistry and Physics*, 22(14), 9601–9616. <https://doi.org/10.5194/acp-22-9601-2022>

White, E. D., Rigby, M., Lunt, M. F., Luke Smallman, T., Comyn-Platt, E., Manning, A. J., Ganesan, A. L., O'Doherty, S., Stavert, A. R., Stanley, K., Williams, M., Levy, P., Ramonet, M., Forster, G. L., Manning, A. C., & Palmer, P. I. (2019). Quantifying the UK's carbon dioxide flux: An atmospheric inverse modelling approach using a regional measurement network. *Atmospheric Chemistry and Physics*, 19(7). <https://doi.org/10.5194/acp-19-4345-2019>

10. History of the document

Version	Author(s)	Date	Changes
V 1.0	Karina Adcock	05/12/2025	New document
	Matt Rigby	15/12/2025	Inversion methodology added
	S. Walter	19/12/2025	Final formatting and upload